Nonlinear rocking dynamics of pre-tensioned single rigid blocks under harmonic base excitation

IOP Conf. Series: Journal of Physics: Conf. Series **1264** (2019) 012006 doi:10.1088/1742-6596/1264/1/012006

Nonlinear rocking dynamics of pre-tensioned single rigid blocks under harmonic base excitation

E Ahmadi, M M Kashani

University of Southampton, Faculty of Engineering and Physical Sciences, Southampton, SO17 1BJ, UK

E.ahmadi@soton.ac.uk

Abstract. The rocking mechanism has been widely recognized as a beneficial technique to reduce structural damage arising from lateral excitations particularly earthquake loading, and hence, segmental pre-tensioned bridge piers have been recently emerged due to their self-centring property accompanied by accelerated construction of such structures. Hence, this study formulates the rocking dynamics of tied pre-tensioned single rigid blocks as an initial study for better understanding of dynamics of segmental pre-tensioned bridge piers. The nonlinear equation of rocking motion is then numerically solved under different range of base harmonic excitations. To achieve this, the rocking initiation condition is considered to determine initial conditions of rocking motion, an implicit solution is adopted to solve the equation of rocking motion and determine rocking response. Finally, a study is performed on a specific composite tied block to investigate effects of geometry and initial pre-tensioning force of the cable on the dynamic behaviour of the block. This study can find use in better understanding of segmental pre-tensioned columns.

1. Introduction

Bridges are inseparable parts of all transport networks, and breakdown of such structures can result in heavy economic damages and numerous life losses. Such damages could be even worse in highly seismic regions particularly for deteriorated and aged bridges where earthquake loading can induce permanent structural damages ([1], [2]). For integral bridges where bridge piers are monolithically connected to both foundation and deck, bridge piers crack due to lateral loading and as a result, accelerated deteriorations occur. Also, very large residual deformations are formed in integral bridges under earthquake loading leading to non-functional structures after seismic events. As a solution to these deficiencies, many studies have been carried out to develop precast structural systems that are constructed using more durable materials, are seismically resilient, and can be used in accelerated bridge construction (ABC) ([3],[4]). Hence, segmental pre-tensioned bridge piers are promising substitutions to conventional monolithic bridges ([5],[6]). The pier segments providing rocking mechanism not only allow for offsite manufacturing which speeds up construction time (i.e. ABC), but also minimise the residual displacement of the pier under lateral dynamic loading (i.e. seismically resilient). Since the pier segments are modelled as tied rigid bodies, a literature survey on the dynamics of rigid blocks better demonstrates the necessity for study rocking dynamics of pre-tensioned single blocks.

The rocking mechanic of rigid blocks is an extensively recognized and investigated subject in the literature. The rocking behavior of single rigid blocks under base excitations were much studied in [7]-

[11]. Previous studies also focused on nonlinear behavior of single rigid blocks under earthquake ground motions ([12]-[15]). Particularly, Simoneschi et al. ([16]-[18]) studied effects of mass dampers on the rocking response mitigation of single rigid blocks under earthquake ground motions. In some studies, single and assemblies of rigid blocks were used to represent dynamic behavior of art objects, and their stability and detailed formulation of sliding and rocking motions were derived and discussed under impulse base excitation ([19]-[21]). All studies mentioned so far addressed nonlinear dynamic of *free-standing* single or assemblies of rigid blocks and no cable or tendon was used to tighten rigid block/blocks. In a unique study, Alexander et al. [22] formulated dynamic of a single *pre-tensioned* rigid block on an elastic foundation. However, the formulation was derived for a class of moment resisting frames, and effect of the block mass was ignored. Further, only small rotations were considered while large rotations can impose higher geometric nonlinearities into the equation of motion. As an extension to Alexander et al.'s work [22], Kashani et al. [23] experimentally investigated a novel class of self-centering bridge columns. Clearly then, the literature lacks rocking formulation of pre-tensioned single blocks, which are very beneficial in better understanding of rocking dynamics of segmental pre-tensioned bridge columns.

The preceding literature survey demonstrates that although rocking dynamics of free-standing rigid blocks have been comprehensively investigated and formulated, formulation of nonlinear rocking dynamics of single tied rigid blocks are yet to be mathematically described and analysed for in depth understanding of dynamic of segmental pre-tensioned bridge piers. Therefore, there is a need for formulation and analysis of single tied blocks under base excitations and this study addresses this knowledge gap. To achieve this goal, kinematic and energy equations are combined together, and a general equation of rocking motion is derived for rocking behaviour of single tied blocks. The rocking initiation condition is considered to determine initial conditions of rocking motion and a numerical algorithm is employed to solve the equation of rocking motion and determine rocking responses. Finally, a study is performed on a specific composite tied block to investigate effects of geometry and initial pre-tensioning force of the cable on the dynamic behaviour of the block.

2. Formulation of rocking motion of a tied block

2.1. Kinematic equations

The horizontal and vertical translation of the centre of gravity of a rigid block which rocks around pivot point o at distance αb from the centre of the block (see figure 1) are determined in this section. The clockwise rocking is taken positive (see figures 1a and 1c), and the block angle, β, and rocking radius, R, are defined as:

$$\beta = -\tan^{-1}\left(2\alpha b / h\right); \quad R = \sqrt{\alpha^2 b^2 + h^2 / 4} \tag{1}$$

Positive β corresponds to the rocking centre on the left-hand side ($\alpha < 0$) (see figure 1a). For positive rocking, α is 0.5 while for negative rocking α is -0.5. The translation vector of the centre of gravity, GG', for a right-hand coordinate system (see figure 1a) is determined from:

$$\overrightarrow{GG'} = \overrightarrow{OG'} - \overrightarrow{OG} \tag{2}$$

Using equation (2) for both positive and negative rocklings (figures 2a and 2b) and some simplifications result in:

$$\overrightarrow{GG'} = \left(R\sin\left(\beta+\theta\right)+\alpha b\right)\vec{i} + \left(R\cos\left(\beta+\theta\right)-h/2\right)\vec{j} \tag{3}$$

in which, $\vec{i}$ and $\vec{j}$ are unit direction vectors for horizontal and vertical axes respectively. Equation (3) is compatible with previous works on dynamics of free standing rigid blocks ([17],[18]), which derived the kinematics of free standing rigid blocks separately for positive and negative rocklings. However, equation (3) combines the kinematics of the rigid block for both positive and negative rocking. This

allows for deriving equation of motion generally for both positive and negative rocking. The increase in the cable length is the chord length of the circular segment formed by the rocking angle, θ:

$$\Delta L = 2\alpha b \sin\left(\theta/2\right) \tag{4}$$

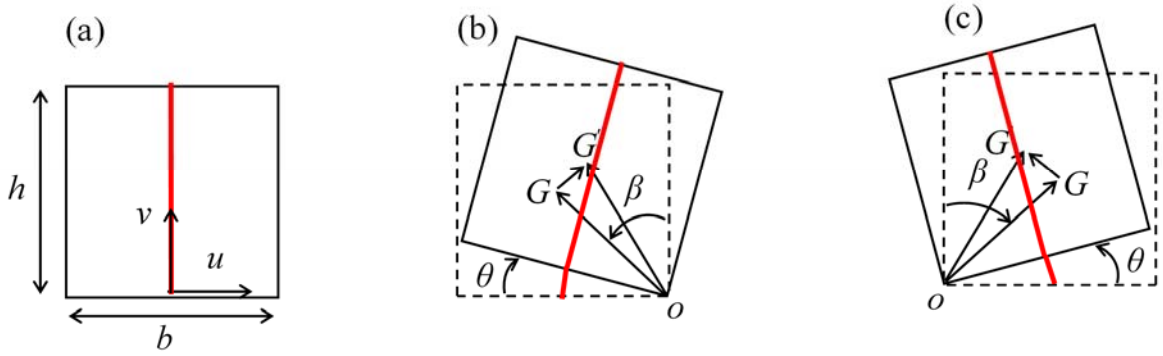

Figure 1. (a) Positive rocking positive rocking ($\theta > 0$) and $\alpha < 0$, and (b) negative rocking ($\theta < 0$) and $\alpha > 0$.

2.2. Energy equations

The energy equation for the system is written as:

$$\frac{d}{dt}\left(\frac{\partial K}{\partial \dot{\theta}}\right) - \frac{\partial K}{\partial \theta} + \frac{\partial \Omega}{\partial \theta} = 0 \tag{5}$$

K is total kinetic energy of the system which is composed of translational energy (K_t) and rocking energy (K_r):

$$K = K_t + K_r = K_u + K_v + K_\theta \tag{6}$$

in which kinetic energies of horizontal and vertical translations as well as angular rocking (K_u, K_v, and K_θ) are given by:

$$K_u = \frac{1}{2} m\left(\dot{u} + \dot{u}_g\right)^2 \tag{7}$$

$$K_v = \frac{1}{2} m\dot{v}^2 \tag{8}$$

$$K_\theta = \frac{1}{2} I\dot{\Theta}^2 \tag{9}$$

where I is the angular moment of inertia of the block around its centre of mass. Ω is total potential energy of the system which is composed of the strain energy of the pre-tensioned cable (Ω_c) and gravitational potential energy of the block (Ω_b):

$$\Omega = \Omega_c + \Omega_b \tag{10}$$

The unstretched and stretched lengths of the cable are:

$$L_0 = h - F_{c0}/k_c \tag{11}$$

and,

$$L_c = h + 2\alpha b \sin\left(\theta/2\right) \tag{12}$$

The strain energy of the pre-tensioned cable is thus determined from:

$$\Omega_c = \frac{1}{2} k_c \left(L_c - L_0\right)^2 = \frac{1}{2} k_c \left(2\alpha b \sin\left(\theta/2\right) + F_{c0}/k_c\right)^2 \tag{13}$$

The gravitational potential energy of the blocks is given by:

$$\begin{aligned}\Omega_b &= mg\left(v - v_0\right) \\ &= mg\left(R\cos\left(\beta+\theta\right) - h/2\right)\end{aligned} \tag{14}$$

2.3. Equation of rocking motion

In this section, equation of rocking motion is derived combining kinematic and energy equations. Regarding partial derivatives of kinetic energies with respect to θ and $\dot{\theta}$, chain rule is used to calculate derivatives of some terms. Using equations (3), (13), and (14), substituting into equations (7)-(9), and simplifying the terms result in:

$$\frac{\partial K_u}{\partial \theta} = -mR\dot{\theta}\sin\left(\beta+\theta\right)\left[R\dot{\theta}\cos\left(\beta+\theta\right) + \dot{u}_g\right] \tag{15}$$

$$\frac{\partial K_v}{\partial \theta} = mR^2\dot{\theta}^2\cos\left(\beta_k+\theta\right)\sin\left(\beta_k+\theta\right) \tag{16}$$

$$\frac{\partial K_\theta}{\partial \theta} = \frac{\partial}{\partial \theta}\left(\frac{1}{2}I\dot{\theta}^2\right) = 0 \tag{17}$$

$$\frac{\partial K_u}{\partial \dot{\theta}} = mR\cos\left(\beta+\theta\right)\left[R\dot{\theta}\cos\left(\beta+\theta\right) + \dot{u}_g\right] \tag{18}$$

$$\frac{\partial K_v}{\partial \dot{\theta}} = mR^2\dot{\theta}\sin^2\left(\beta+\theta\right) \tag{19}$$

$$\frac{\partial K_\theta}{\partial \dot{\theta}} = \frac{\partial}{\partial \dot{\theta}}\left(\frac{1}{2}I\dot{\theta}^2\right) = I\dot{\theta} \tag{20}$$

$$\frac{\partial \Omega_b}{\partial \theta} = -mgR\sin\left(\beta+\theta\right) \tag{21}$$

$$\frac{\partial \Omega_c}{\partial \theta} = \alpha k_c b\cos\left(\theta/2\right)\left[2\alpha b\sin\left(\theta/2\right) + F_{c0}/k_c\right] \tag{22}$$

Substituting equations (15)-(22) into energy equation (equation (5)) results in the equation of the rocking motion for the block:

$$\Gamma = I_o\ddot{\theta} + \alpha k_c b\cos\left(\theta/2\right)\left[2\alpha b\sin\left(\theta/2\right) + F_{c0}/k_c\right] - mgR\sin\left(\beta+\theta\right) + mR\cos\left(\beta+\theta\right)\ddot{u}_g = 0 \tag{23}$$

where $I_O = I + mR^2 = \frac{4}{3}mR^2$ is the angular inertia of the block around the rocking centre.

3. Uplift condition and numerical solution

3.1. Rocking initiation

Consider a single tied block rocking around its pivot point *o* (figures 2a and 2b). It is assumed that sliding does not exist due to the pre-tensioned cable and high static friction coefficient. Using equation (23) and setting $\ddot{\theta} = 0$ and $\ddot{u}_g = 0$, the remaining terms reflect static moment-rotation relationship for a single tied block:

$$M\left(\theta\right) = \alpha k_c b\cos\left(\theta/2\right)\left[2\alpha b\sin\left(\theta/2\right) + F_{c0}/k_c\right] - mgR\sin\left(\beta+\theta\right) \tag{24}$$

Figure 2c shows the moment-rotation of a single tied block. The static moment comes from the gravitational force of the block and the pre-tensioned cable. The block has an infinite rocking stiffness

until the magnitude of the applied moment reaches value of αbF_{c0}-$mgR\sin\beta$, and from this point onwards, the block starts rocking, and the rocking stiffness changes nonlinearly as the rocking increases, i.e. geometrically nonlinear. During rocking, the moment-rotation relationship follows the same trend without any energy loss due to ignoring friction (no sliding) and impact when the angle of rotation reverses. Under a positive ground motion (from the left to the right), the block will start rocking in the negative direction as the inertia force due to base excitation tends to overturn the block (i.e. overturing moment) and the gravity force of the block and tension force of the cable will resist against overturning, i.e. resisting moment (see figure 2b). Thus, the positive rocking will happen under the negative base excitation (from the right to left).

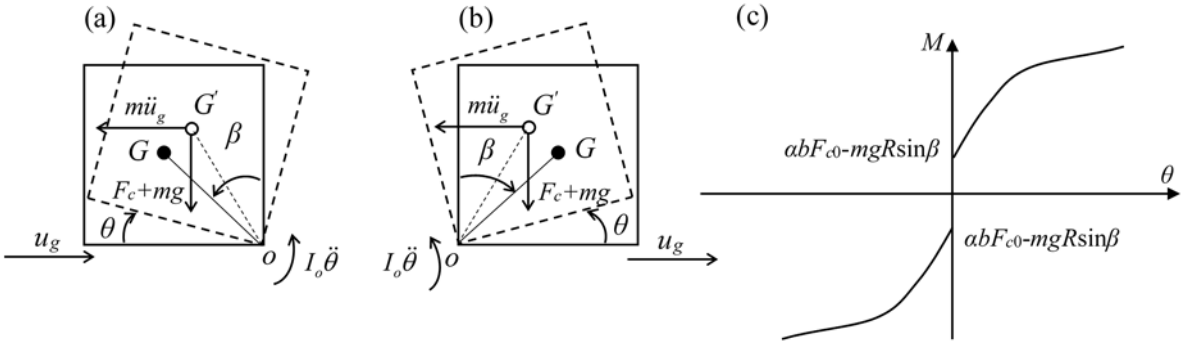

Figure 2. Free-body diagram of a single block: (a) θ>0, and (b) θ<0, and (c) moment-rotation relationship of a single block.

At the time of rocking initiation (t = 0 and θ = 0) under a positive base excitation, the block is in vertical equilibrium and the minimum ground acceleration required for the rocking initiation is obtained from the condition:

$$m\left|\ddot{u}_g\right| R\cos\beta \geq \left(mg + F_{c0}\right) R\sin\beta \rightarrow \left|\ddot{u}_g^{\min}\right| = \left(g + F_{c0}/m\right)\tan\beta \tag{25}$$

Substituting $\theta = 0$ at $t = 0$ and minimum ground acceleration from equation (24) into equation (23) gives $\ddot{\theta}(0) = 0$. The initial condition of the block after transition phase (e.g. from positive to negative rocking or vice versa) is $\theta^-\left(t_i^-\right) = \theta^+\left(t_i^+\right) = 0$ and $\dot{\theta}^+\left(t_i^+\right) = \dot{\theta}^-\left(t_i^-\right)$. Note that it is assumed that no energy is consumed during the transition. Substituting these conditions into the equation of rocking motion gives the angular acceleration after impact $\ddot{\theta}^+\left(t_i^+\right)$.

3.2. Numerical solution

To solve equation (23) numerically, a numerical algorithm shown in figure 3 is used. The block is stationary before any external excitation, and thus angular displacement, velocity, and acceleration at time zero (j = 0 where j is the time counter) are all zero, $\theta^0 = \dot{\theta}^0 = \ddot{\theta}^0 = 0$. To calculate the response of the system for the next time, j+1, Newton-Raphson and Newmark methods are simultaneously implemented [3]. The nonlinearity in the equation (23) is expressed as a residual moment due to the unbalance of internal and external moments. The residual moment at the current time, (j+1)Δt of the dynamic system is defined as $\Delta\left[\Gamma\right]^{(j+1)\Delta t}$. At the current time, ($j$+1)$\Delta t$, the null angular acceleration, $\ddot{\tilde{\theta}}_0^{(j+1)\Delta t} = 0$, is assumed for the initial guess, and accordingly following equations from Newmark method are used to determine initial angular displacement and velocity for the current time using responses of the previous time, j,:

$$\begin{aligned}\dot{\tilde{\theta}}_0^{(j+1)\Delta t} &= \dot{\theta}^{j\Delta t} + \left(1-\gamma\right)\ddot{\theta}^{j\Delta t}\Delta t \\ \tilde{\theta}_0^{(j+1)\Delta t} &= \theta^{j\Delta t} + \dot{\theta}^{j\Delta t}\Delta t + \left(0.5-\lambda\right)\ddot{\theta}^{j\Delta t}\Delta t^2\end{aligned} \tag{26}$$

where $\gamma = 0.5$ and $\lambda = 0.25$ which is unconditionally stable.

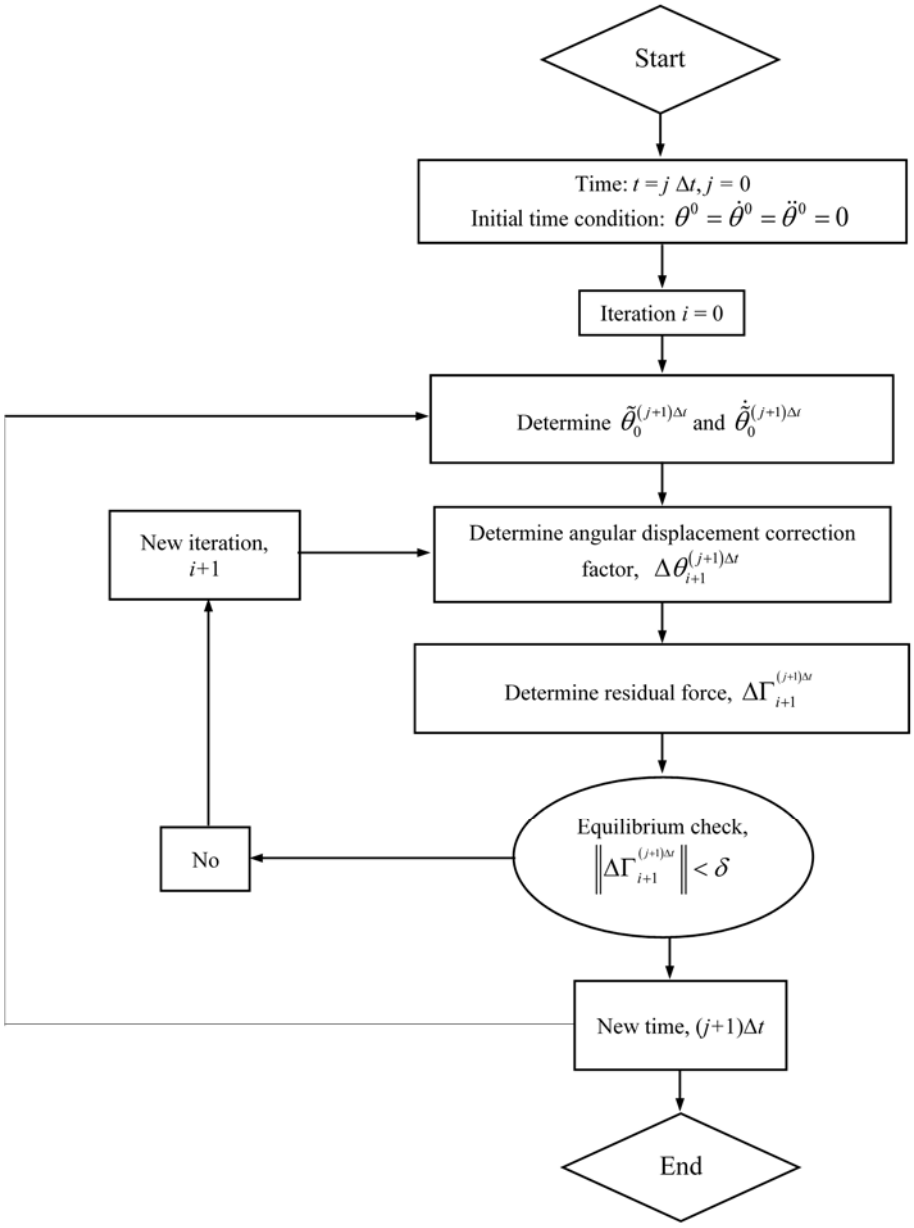

Figure 3. Algorithm used for numerical analysis of the nonlinear rocking equation of motion.

The residual moment is linearized at the current time, $(j+1)\Delta t$ and enforced to be zero using the first two terms of its Taylor's series for the iteration $i+1$ leading to angular displacement correction factor, $\Delta\theta_{i+1}^{(j+1)\Delta t}$. Angular displacement, velocity, and acceleration are updated for the iteration $i+1$ using the angular displacement correction factor:

$$\ddot{\theta}_{i+1}^{(j+1)\Delta t} = \left(\frac{1}{\lambda\Delta t^2}\right)\Delta\theta_{i+1}^{(j+1)\Delta t}$$

$$\dot{\theta}_{i+1}^{(j+1)\Delta t} = \dot{\tilde{\theta}}_0^{(j+1)\Delta t} + \left(\frac{\gamma}{\lambda\Delta t}\right)\Delta\theta_{i+1}^{(j+1)\Delta t}$$

$$\theta_{i+1}^{(j+1)\Delta t} = \tilde{\theta}_0^{(j+1)\Delta t} + \Delta\theta_{i+1}^{(j+1)\Delta t} \tag{27}$$

and, then the residual moment is determined for the iteration i+1 at the current time. The norm of the residual moment vector is calculated and compared with the tolerance, δ. If the norm is larger than the tolerance, new iteration is performed at the current time until the norm falls less than the tolerance (Newton-Raphson method), and the same procedure is repeated for the next time instant.

4. Exemplar results for harmonic excitation

In this section, the results are presented for a specific tied block under harmonic excitation. The block section is a glass fibre reinforced polymer (GFRP) box section filled with fibre concrete and tightened by an GFRP bar (see figure 4). This section is chosen as it will be used in large-scale experimental testing of a novel segmental pre-tensioned bridge column by the authors. The section is 100×100 mm and has mass per unit length, ρ, 2.265e-3 kg/mm. The GFRP bar diameter is taken 13 mm with elastic modulus of 63500 MPa.

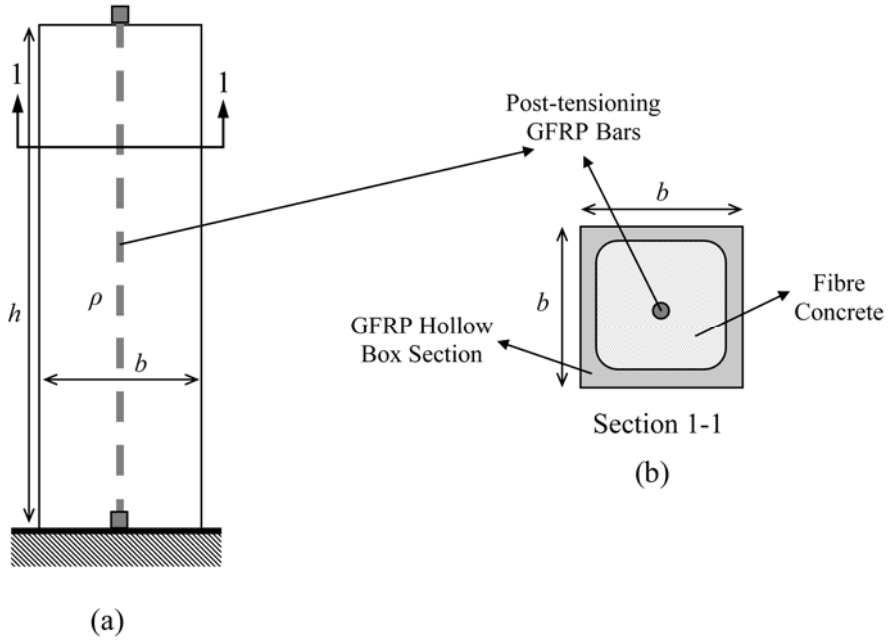

Figure 4. (a) Composite pre-tensioned block, and (b) block section details.

In the following, a parametric analysis is performed on the block's height, h, and the bar's pre-tensioned force, F_{c0}, for a range of excitation frequencies. Figure 5 shows time histories of angular displacement, angular velocity, and angular acceleration of a bock with h = 500 mm, and F_{c0} = 5000 N for a frequency excitation of 5 Hz and an amplitude of 0.5g. The time histories show a steady-state response for angular displacement, velocity, and acceleration. However, unlike responses of linear systems, the temporal shape of the responses for the tied block is not a typical sine-like response under harmonic excitations. This mainly comes from geometric nonlinearities of the system which makes the response different from a harmonic-like response. In this example, the maximum angular displacement of the block, θ_{max}, is 0.054 rad. In the following, maximum angular displacement are determined for a frequency range of 1-10 Hz with increment of 1 Hz. For cases where frequencies lower than 1 Hz is required, a frequency range of 0.1-1 Hz with increment of 0.1 Hz is also considered.

To see the effects of initial pre-tensioning force on vibration response of the tied blocks, maximum angular displacement versus excitation frequency are plotted in figure 6 for a block of h = 500 mm with F_{c0} values of 0 kN, 2 kN, 5 kN, and 10 kN. As seen, the initial pre-tensioning force does not significantly affect the dynamic response of the block. Further, the response approaches very large undesirable values in a frequency range of 0.5-0.8 Hz which shows the resonant frequency range of the tied block. It should be noted that initial pre-tensioning force has a negligible effects on this range of resonant frequency.

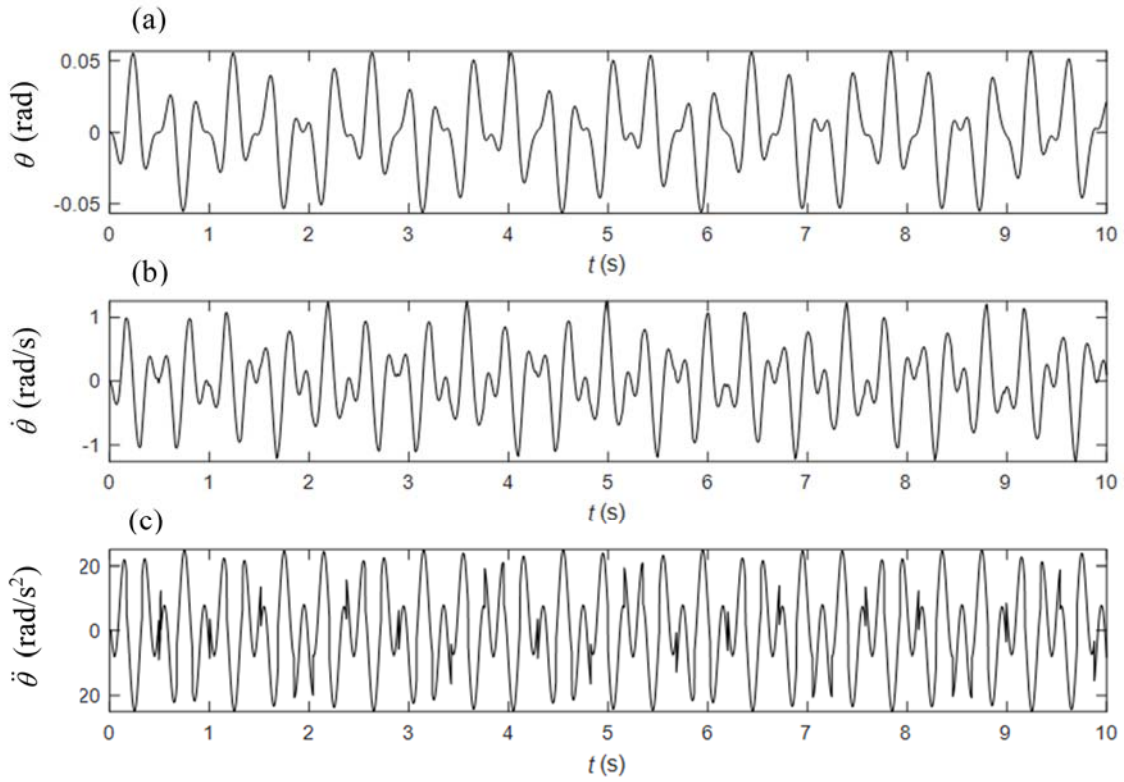

Figure 5. Time-history analysis: (a) angular displacement, (b) angular acceleration, and (c) angular acceleration.

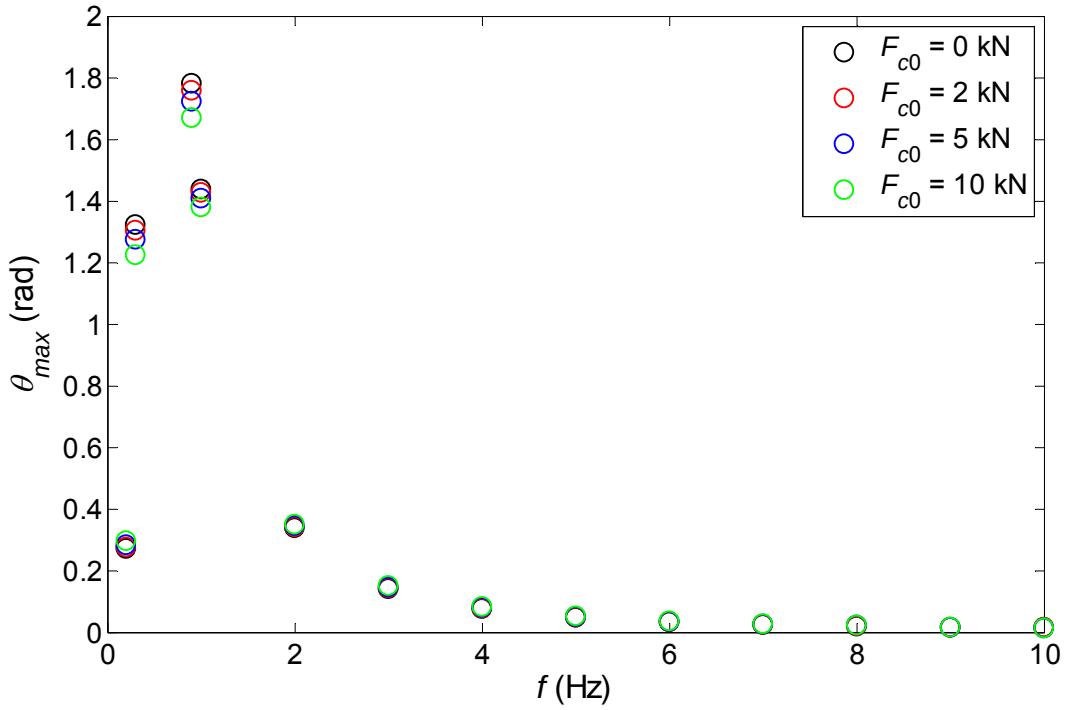

Figure 6. Maximum angular displacement versus excitation frequency for blocks with h = 500 m and different initial pre-tensioning forces.

To investigate the effects of the block's height on vibration response of the system, maximum angular displacement versus excitation frequency are plotted in figure 7 for a block of $F_{c0} = 0$ kN with h values of 200 mm, 350 mm, and 500 mm. As the block's height increases, the system's stiffness reduces, and consequently the system's response increases around the range of resonant frequency. Additionally, the range of resonant frequency shifts toward higher frequencies as the blocks becomes squatter. The resonant frequency range is around 2 Hz and 7 Hz respectively for blocks of height 350 mm and 500 mm.

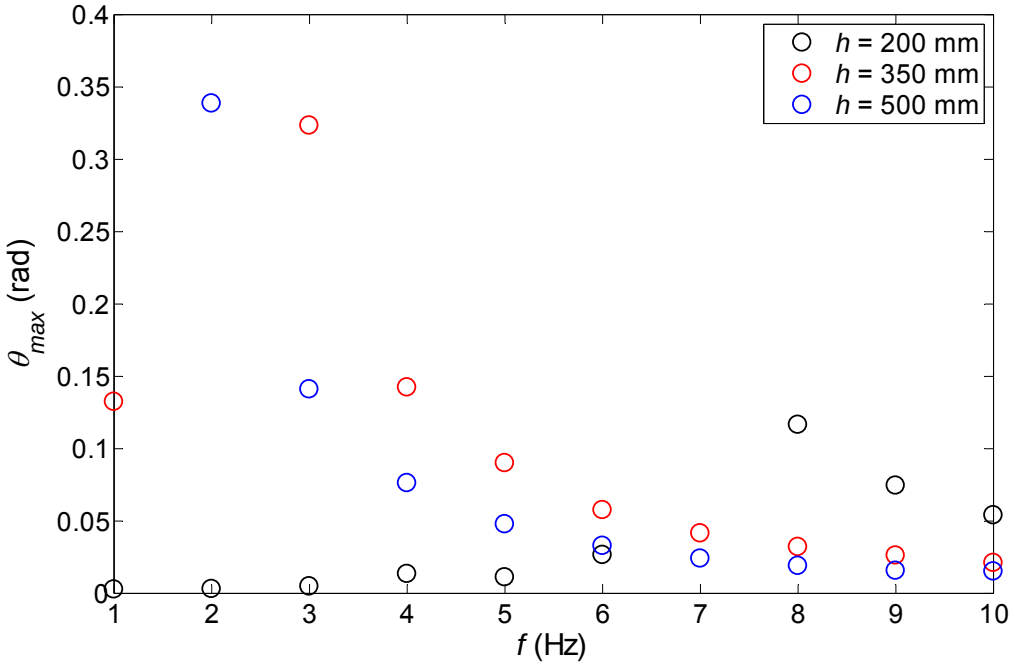

Figure 7. Maximum angular displacement versus excitation frequency for blocks with $Fc0 = 0$ kN and different heights.

5. Conclusions

In this study, the nonlinear rocking motion of the tied single block was derived and numerically solved for the first time. To achieve this goal, kinematic and energy equations were combined together and nonlinear rocking motion of the system was formulated. A Newmark method merged with Newton-Raphson scheme was adopted to numerically solve the rocking equation derived. The dynamic response was determined for a composite block with different heights and initial pre-tensioning force. A resonant frequency range was observed which was not affected by the initial pre-tensioning force. However, the block's height increases this resonant frequency range as the squat blocks have a higher stiffness. The derived equation can be extended to multiple pre-tensioned blocks and solved which can find use in better understanding of pre-tensioned segmental rocking columns.

6. Acknowledgment

The authors acknowledge support received by the UK Engineering and Physical Sciences Research Council (EPSRC) for a Prosperous Nation [grant number EP/R039178/1**:** *SPINE: Resilience-Based Design of Biologically Inspired Columns for Next-Generation Accelerated Bridge Construction*].

References

[1] Kashani MM, Crewe AJ and Alexander NA 2017 Structural capacity assessment of corroded RC bridge piers *Proceedings of the Institution of Civil Engineers: Bridge Engineering* **170**(1):28-41.

[2] Kashani MM, Lowes LN, Crewe AJ and Alexander NA 2016 Computational modelling strategies for nonlinear response prediction of corroded circular RC bridge piers *Advances in Materials Science and Engineering* **2016** doi:10.1155/2016/2738265.
[3] Tazarv M and Saiidi MS 2016 Low-damage precast columns for accelerated bridge construction in high seismic zones *Journal of Bridge Engineering* **21** doi:10.1061/(ASCE)BE.1943-5592.0000806.
[4] Haber ZB 2013 Precast column-footing connections for accelerated bridge construction in seismic zones, *ProQuest Dissertations and Theses*.
[5] Shim CS, Chung CH and Kim HH 2008 Experimental evaluation of seismic performance of precast segmental bridge piers with a circular solid section *Engineering Structures* **30**:3782–3792 doi:10.1016/j.engstruct.2008.07.005.
[6] Dawood H, ElGawady M and Hewes 2012 Behavior of segmental precast posttensioned bridge piers under lateral loads *Journal of Bridge Engineering* **17**:735–746 doi:10.1061/(ASCE)BE.1943-5592.0000252.
[7] Spanos PD and Koh AS 1985 Rocking of rigid blocks due to harmonic shaking *ASCE Journal of Engineering Mechanics* **110**:1627–1642.
[8] Spanos PD and Koh AS 1986 Analysis of block random rocking *Soil Dynamics and Earthquake Engineering* **5**:178–183 doi:10.1016/0267-7261(86)90021-7.
[9] Shenton HW and Jones NP 1991 Base excitation of rigid bodies I: formulation *Journal of Engineering Mechanics* **117**:2286–2306 doi:10.1061/(ASCE)0733-9399(1991)117:10(2286).
[10] Shenton HW and Jones NP 1991 Base excitation of rigid bodies II: periodic slide-rock response *Journal of Engineering Mechanics* **117**:2307–2328 doi:10.1061/(ASCE)0733-9399(1991)117:10(2307).
[11] Kounadis AN 2013 Parametric study in rocking instability of a rigid block under harmonic ground pulse: A unified approach *Soil Dynamics and Earthquake Engineering* **45**:125–143. doi:10.1016/j.soildyn.2012.10.002.
[12] Yim CS, Chopra AK nad Penzien J 1980 Rocking response of rigid blocks to earthquakes *Earthquake Engineering and Structural Dynamics* **8**:565–587 doi:10.1002/eqe.4290080606.
[13] Aslam M, Godden WG and Scalise DT 1980 Earthquake rocking response of rigid bodies *Journal of Structural Division* **106**:377–392.
[14] Pompei A, Scalia A and Sumbatyan MA 1998 Dynamics of rigid block due to horizontal ground motion *Journal of Engineering Mechanics* **124**:713–717 doi:10.1061/(asce)0733-9399(1998)124:7(713).
[15] Taniguchi T 2002 Non-linear response analyses of rectangular rigid bodies subjected to horizontal and vertical ground motion *Earthquake Engineering and Structural Dynamics* **31**:1481–1500. doi:10.1002/eqe.170.
[16] de Leo AM, Simoneschi G, Fabrizio C and Di Egidio A 2016 On the use of a pendulum as mass damper to control the rocking motion of a rigid block with fixed characteristics *Meccanica* **51**:2727–2740 doi:10.1007/s11012-016-0448-5.
[17] Simoneschi G, de Leo AM and Di Egidio A 2017 Effectiveness of oscillating mass damper system in the protection of rigid blocks under impulsive excitation *Engineering Structures* **137**:285–295 doi:10.1016/j.engstruct.2017.01.069.
[18] Simoneschi G, Geniola A, de Leo AM nad Di Egidio A 2017 On the seismic performances of rigid block-like structures coupled with an oscillating mass working as a TMD *Earthquake Engineering and Structural Dynamics* **46**:1453–1469 doi:10.1002/eqe.2864.
[19] Kounadis AN 2015 On the rocking-sliding instability of rigid blocks under ground excitation: some new findings *Soil Dynamics and Earthquake Engineering* **75**:246–258 doi:10.1016/j.soildyn.2015.03.026.
[20] Kounadis AN and Papadopoulos GJ 2016 On the rocking instability of a three-rigid block system under ground excitation *Archive of Applied Mechanics* **86**:957–977 doi:10.1007/s00419-015-1073-9.

[21] Kounadis AN 2018 The effect of sliding on the rocking instability of multi- rigid block assemblies under ground motion *Soil Dynamics and Earthquake Engineering* **104**:1–14 doi:10.1016/j.soildyn.2017.03.035.
[22] Alexander AN, Oddbjornsson O, Taylor CA, Osinga HM and Kelly DE 2011 Exploring the dynamics of a class of post-tensioned, moment resisting frames *Journal of Sound and Vibration* **330**:3710–3728 doi:10.1016/j.jsv.2011.02.016.
[23] Kashani MM, Gonzalez-Buelga A., Thayalan RP, Thomas AR., and Alexander NA 2018 Experimental investigation of a novel class of self-centring spinal rocking column. *Journal of Sound and Vibration* **437**:308-324.